Nanoscale

Accepted Manuscript

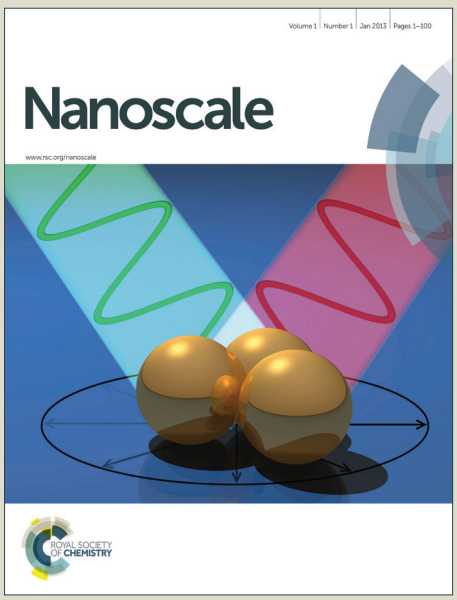

ROYAL SOCIETY OF CHEMISTRY

www.rsc.org/nanoscale

Nanoscale

RSCPublishing

COMMUNICATION

One-step formation of responsive "dumbbell" nanoparticle dimers via quasi-two-dimensional polymer single crystals

Cite this: DOI: 10.1039/x0xx00000x

Tian Zhou,[a] Bin Dong,[a,b] Hao Qi,[a] Hang Kuen Lau,[a] and Christopher Y. Li[a*]

Received,

DOI: 10.1039/x0xx00000x

www.rsc.org/

We present a facile approach to synthesize "dumbbell" nanoparticle dimers via one-step coupling of nanoparticles and quasi-two dimensional polymer single crystals. These dimers exhibit responsive properties enabled by flexible polymeric linkers.

Forming nanoparticle (NP) assembles (or hetero NP clusters), such as dimers, trimers or chains, has led to enhanced NP performance and value-added properties.[1] In general, controlled nucleation and growth methods can be used to fabricate NP ensembles with solid-state interface while ligand coupling approaches produces NP ensembles with organic linkers.[2] Moreover, since the properties of NP dimers are strongly coupled with the gap distance between the bonded NPs, it is of great interest to synthesize NP dimers with a tunable gap distance. Controlled hybridization of DNA strands has been demonstrated to tune the gap distance of NP dimers.[3] However, the overall process is relatively costly and difficult to handle. Other reported works on the synthesis of NP dimers with organic linkers often require multiple functionalization steps; therefore, developing a simple and versatile approach for NP dimer synthesis remains a challenging task.

Herein, we report a facile method to synthesize responsive NP dimers based on a polymer-single-crystal-templating (PSCryT) method. Exploiting the different chemical structures of the polymer chain ends and backbone, previous studies have shown that, quasi-two-dimensional (2D) polymer single crystals (PSCs) can be obtained with chain ends excluded on the lamellar surface by carefully controlling the crystallization condition.[4] These organic groups can serve as "acceptors" for immobilization of different NPs via chemisorption. By so doing, a "nanosandwich" structure with NPs covering both sides of the PSC can be obtained.[5] In the present study, we show that when α, ω-end functionalized poly(ε -caprolactone) (PCL) is used to grow PSCs (Scheme 1), and when crystallization conditions are carefully controlled, an *extended* chain conformation is formed with both functional groups of one chain "pinned" at the *opposite* surfaces of the PSC. One-step coupling of this PSC with NPs leads to NP dimers with PCL as the covalent linkers. Since the polymer ends can be readily functionalized, numerous NP systems can be used for dimerization. Moreover, the conformational change of the polymer linker can directly lead to varied gap distances, which renders the NP dimers with interesting responsive properties.

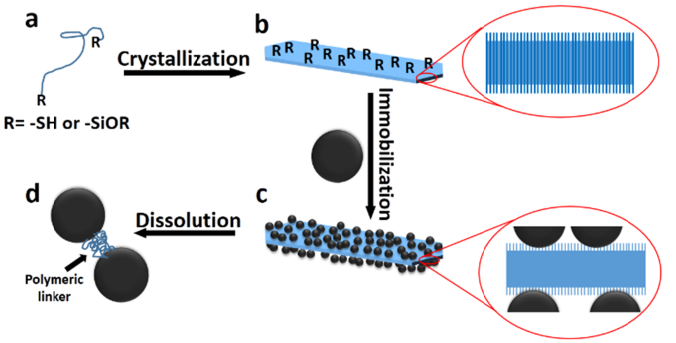

Scheme 1. Synthesis route of nanoparticle dimers via the PSCryT method: a. α, ω-difunctionalized polycaprolactone (PCL) with thiol (-SH) or alkoxysilane (-SiOR) terminal groups; b. PCL single crystals with functional chain ends covering the lamellae surface; the enlarged scheme demonstrates the extended chain conformation within lamellae; c. nanoparticle-decorated PCL single crystals; d. nanoparticle dimers with polymer linkers after dissolving the single crystals.

In this study, bifunctional, hydroxyl-terminated PCL ($PCL(OH)_2$, $M_n \sim 2k$ g/mol) was used as a model polymer. The hydroxyl chain ends of $PCL(OH)_2$ were functionalized with 3-mercaptopropionic acid and 3-(triethoxysilyl)propyl isocyanate to yield thiol- or alkoxysilane-terminated PCL. The completion of chain functionalization was monitored using NMR (Figure S1). The resultant $PCL(SH)_2$ and $PCL(SiOR)_2$ were used to grow PSCs in 1-butanol at 35 °C following a self-seeding method. Figure 1 shows AFM images of the two different PSCs and the corresponding height profile. The $PCL(SH)_2$ PSC shows a hexagonal shape with six distinct facets while $PCL(SiOR)_2$ PSCs are leaf-like. This morphological difference can be attributed to the surface energy difference of single crystals. Both of these crystals have a similar average thickness of 14 nm according to the AFM height profile. On the basis of lamellar thickness, the PCL unit cell parameters,[6] and the degree of polymerization (DP ~ 16 based on NMR results, see Figure S1), we can conclude that an extended-chain conformation is formed in these lamellar crystals, and the two

functional groups of one single chain are excluded onto the opposite sides of the crystal surface, as shown in Scheme 1. This structure is ideal for the NP dimer synthesis because it provides 1) a maximum number of available adsorption sites on the lamellar surface, ~ 5.4 groups/nm^2, and 2) the highest possibility for coupling two NPs on the opposite ends of one single chain.

These functionalized quasi-2D PSCs were then incubated with various NP solutions as described in the experimental section. PCL(SH)$_2$ PSCs were used as a model system to immobilize Fe_3O_4NPs (~ 12 nm in diameter), and the obtained "nanosandwich" structure is denoted as PCL(SH)$_2$SC@Fe_3O_4NPs. To achieve a high yield of dimers, dense nanoparticle coverage is critical. In this study, four consecutive chemisorption processes were applied and Figure 2a,b shows the PSCs after the fourth attachment. Approximately 45.7% of the projected single crystal fold surface is covered with Fe_3O_4NPs. Figure S2 shows the coverage is approximately 11.2% to 39.5% after first to third immobilization. Dissolution of these nanosandwiches directly leads to nanoparticle dimers as shown in Figure 2c and Figure S2. Inset of Figure 2c clearly reveals NP that dimers are separated by a small gap. Image analysis of low magnification TEM micrographs show that approximately 48.8% of the NPs are converted to dimers. This relatively high yield is attributed to the dense NP coverage. The conversion is approximately 16.8% and 43.7% after first and third immobilization, respectively (Figure S2).

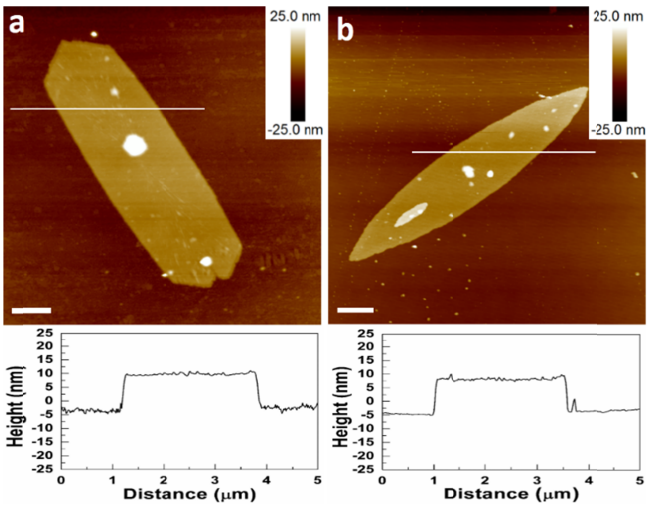

Figure 1. Atomic force microscopy (AFM) images and the corresponding height profiles of PCL(SH)$_2$ (a) and PCL(SiOR)$_2$ (b) single crystal. The scale bars are 1μm.

In addition to Fe_3O_4NPs, gold NPs (AuNPs, 9 nm in diameter) have been immobilized on PCL(SH)$_2$ PSCs, and the resultant nanosandwiches are denoted as PCL(SH)$_2$SC@AuNPs. Figure 2d-f shows PCL(SH)$_2$SC@AuNPs and the corresponding dimers. The particle size distribution of AuNPs immobilized on single crystals is shown in Figure S3. Figure S4 shows high-resolution TEM micrographs of Fe_3O_4NP-dimer and AuNP-dimer revealing the corresponding nanoparticle lattice structures. By changing the terminal groups of PCL, we also can grow PSCs with alkoxysilane surface to immobilize SiNPs (~10-15 nm in diameters). Figure 2g-i shows the PCL(SiOR)$_2$SC@SiNPs nanosandwich and the corresponding SiNP dimers. Both AuNPs and SiNPs form dense NP layers on the PSC lamellar surface after four immobilization processes, leading to high yields of dimers, 53.4% and 51%, respectively. Furthermore, in all the above mentioned dimers, the nanoparticles are covalently bonded via PCL brushes. In order to experimentally support our model, NMR was used to characterize the surface chemical structure of AuNP-dimer nanoparticles. The presence of PCL was confirmed by the appearance of resonance peak around 4.1 ppm (Figure S1c). Furthermore, ruthenium tetroxide (RuO_4) was used to stain AuNP-dimer samples for TEM imaging. Figure 3a shows that before staining, the dimer has a gap of 2-3 nm. After RuO_4 staining, this gap zone becomes gray as shown in Figure 3b, which is because that RuO_4 preferentially stains the PCL domain between AuNPs. Combining the NMR and TEM results, we can conclude that PCL chains are indeed the linkers between the nanoparticle dimers.

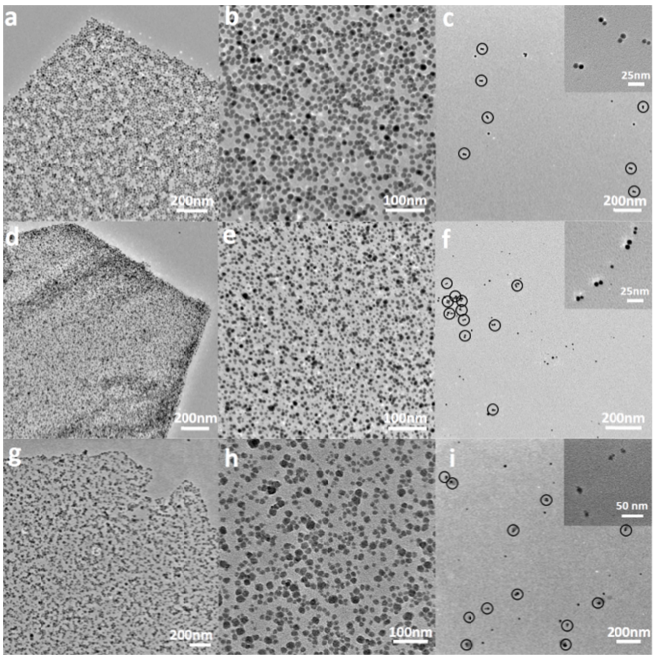

Figure 2. Transmission electron microscopy (TEM) images of polymer single crystal templated nanoparticle sandwiches and the corresponding nanoparticle dimers. a & b: PCL(SH)$_2$@ Fe_3O_4NPs; c: Fe_3O_4NP-dimer nanoparticles; d & e: PCL(SH)$_2$@AuNPs; f: AuNP-dimer nanoparticles; g & h: PCL(SiOR)$_2$@SiNPs; i: SiNP-dimer nanoparticles. Dimer particles in c, f & I were highlighted by black circles. The insets in c, f & i are high magnification TEM images of nanoparticle dimers.

One of the advantages of using flexible polymers linking NPs to form dimers is that polymer conformation, correlated to the gap distance between the dimers, can be easily adjusted via external stimuli. This phenomenon has been successfully demonstrated using DNA sequence as the linker for gold NP dimer synthesis.[7] In the present study, to demonstrate this concept, we choose AuNP dimers as a model system because the Surface Plasmon Resonance (SPR) of AuNPs red shifts and broadens upon dimer formation, and this effect is enhanced when the inter-distance between AuNPs is decreased.[8] Since the conformation of PCL chains can be tuned in solution by adding a non-solvent, simply monitoring the SPR band of the AuNP dimer solution while adding PCL non-solvent would reveal the polymer chain conformation change.

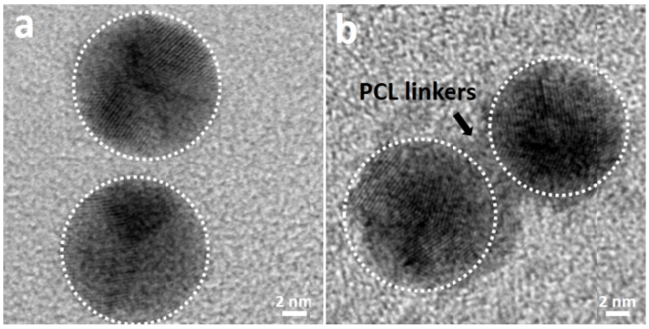

Figure 3. High-resolution transmission electron microscopy (HRTEM) images of AuNP-dimer without staining (a) and with RuO_4 staining (b). The white dotted circles were used to highlight the edge of AuNPs.

Figure 4a shows the UV-Vis spectra of the AuNPs and AuNP dimer solution in toluene. Compared with as-synthesized AuNPs, the SPR band of AuNP dimer solution red-shifts about 6 nm, which can be attributed to both thiol-ligand immobilization on the NP surface and the formation of dimer structure.[9] Also, the absorption band of AuNP-dimer is noticeably broadened - full width at half maximum (FWHM) increased from 57 nm to 62 nm. This can be attributed to the coupling of AuNPs in dimers.[10] Hexane was then gradually added into the dimer solution to trigger the conformational change of PCL chains. The UV-Vis spectra (Figure 4b) show that when the concentration of hexane increased, the SPR band shifts to higher wavelength, and significantly broadens. To rule out the effects of refractive index change with hexane addition, a control experiment was conducted by monitoring the UV-Vis absorption of AuNPs in the mixed solvent of toluene and hexane as shown in Figure 4a. No obvious band shift was found even with 50 vol.% hexane concentration, which confirms that the SPR band shift in AuNP dimers is induced by the optical properties of the dimers in solution. Inset of Figure 4b shows that the band position upshifts from 533 to 540 nm while the FWHM increases from 62 to 69 nm. Moreover, when hexane content is less than 28 vol.%, the red-shift of SPR band and the FWHM increase are relatively slow. Further increasing hexane concentration results in a more rapid change. To better understand this behaviour, DLS experiments were conducted on AuNP dimers in mixed solvent of toluene and hexane as shown in Figure 5. In pure toluene, AuNP solution shows an average hydrodynamic diameter (D_h) of ~ 33 nm for the dimers, and the peak is relative broad, possibly because of a small amount of single AuNPs in the solution. As hexane was gradually added into the solution, D_h first decreased to 28 nm when the volume ratio between toluene/hexane was 5/2. Further adding hexane increased D_h to 100 nm, which remained constant up to 1:1 toluene/hexane ratio. The abrupt transition of D_h at 5/2 toluene/hexane ratio is consistent with the previous discussed SPR results.

The intriguing down-up shifts of the SPR and the DLS results can be attributed to the nature of AuNP dimers. As shown in Scheme 1, for each AuNP dimer, the PCL chains form the covalent linker between the NP, and the rest of the NP surface is covered by a surfactant, didecyldimethylammonium bromide (DDAB). Hexane is a poor solvent for PCL but a good solvent for DDAB. Therefore, the addition of a small amount of hexane triggers the collapse of PCL, which leads to a decreased D_h and weak red-shift and broadening of SPR band as shown in Figure 4. When the concentration of hexane is high, dimers start to aggregate, to prevent the PCL domains from being exposed to solvent. This clustering process thus causes the increase of D_h and a more significant change in the UV-Vis spectrum. The insets in Figure 5 show two representative TEM

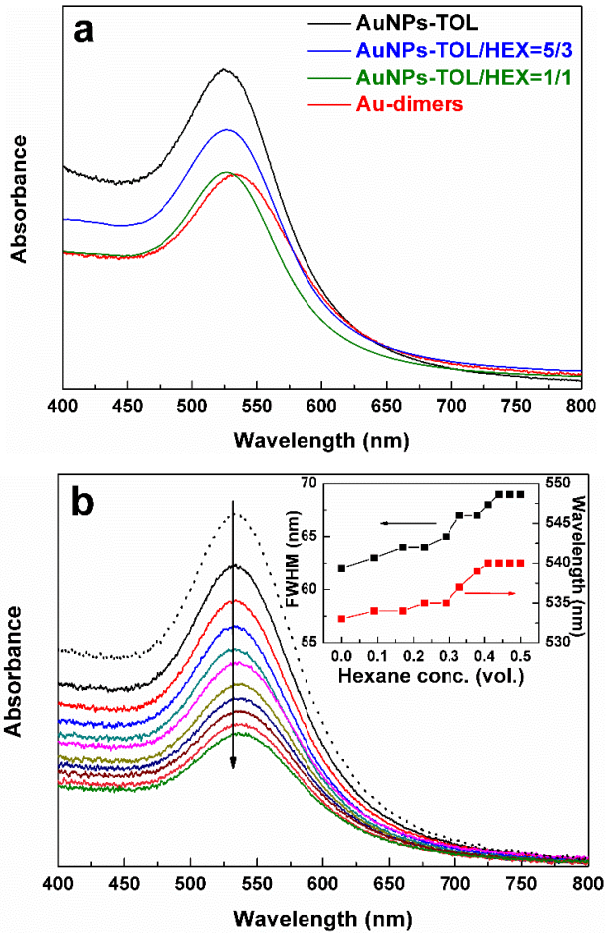

Figure 4. UV-Vis absorption spectra of: a. as-synthesized AuNPs and dimers in toluene, and AuNPs in mixed solvent of toluene (TOL) and hexane (HEX) with different volume ratio; b. gold nanoparticle dimers in pure toluene (dotted line) and mixed solvents with different toluene to hexane volume ratios (solid lines, from 10/1 to 1/1 according to the arrow direction). The inset of b shows the peak position and full width at half maximum (FWHM) of each UV-Vis spectrum with respect to the concentration of hexane in the mixed solvent.

images of AuNP dimers before and after clustering and Figure S5 shows detailed images of AuNP dimers and clusters in six different mixed solvent ratios. It is evident that for samples with toluene/hexane ratios of 5:0, 5:1, and 5:2, dimers are observed and when ratio changed to 5:3, 5:4 and 5:5, clusters with an average size of 100 nm are formed, consistent with the SPR and DLS experiments. Our experiments also show that adding toluene into the 5:5 mixed solvent leads to a redispersion of the clusters and expansion of the dimer size, indicating that the process is reversible.

In summary, we have developed a facile and versatile PSCryT method to synthesize reversibly responsive NP dimer assemblies. Bifunctional PCL is crystallized in solution to afford extended-chain PSCs, which are used as templates to immobilize various NPs, including AuNPs, Fe_3O_4NPs and

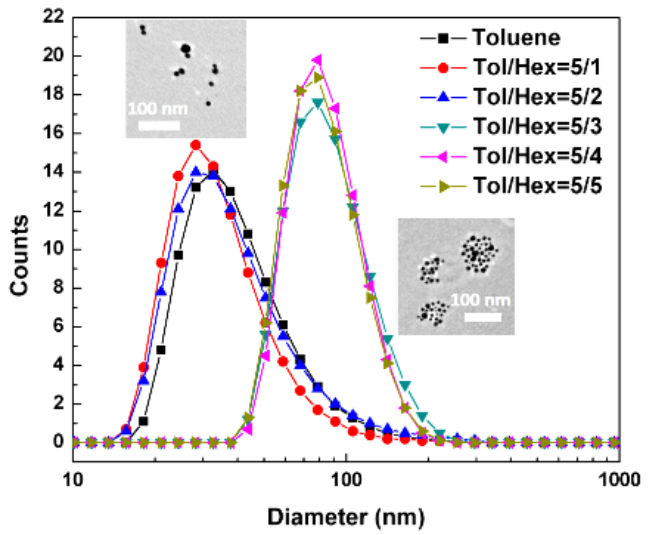

Figure 5. AuNP-dimer size distribution in mixed solvents of toluene (Tol)/hexane (Hex) with different volume ratios. The insets are typical TEM images of AuNP-dimer nanoparticles and clusters formed in solution.

SiNPs. After dense layers of NPs are formed on both sides of the lamellar surface, PCL PSCs are dissolved in solvent to yield NP dimers without further treatment.

Acknowledgements

This work was supported by the NSF (CMMI-1100166 and CMMI-1200385).

Notes and references

[a] Department of Materials Science and Engineering, Drexel University, Philadelphia, Pennsylvania 19104, United States.
*Tel: 215-895-2083, Email: chrisli@drexel.edu
[b] Institute of Functional Nano & Soft Materials (FUNSOM), Soochow University, Suzhou, Jiangsu 215123, China.

Electronic Supplementary Information (ESI) available: Experimental procedure and Figure S1, S2, S3, S4 and S5. See DOI: 10.1039/c000000x/

1. a. C. B. Murray, C. R. Kagan and M. G. Bawendi, *Annu. Rev. Mater. Sci.*, 2000, **30**, 545-610; b. E. Hao and G. C. Schatz, *J. Chem. Phys.*, 2004, **120**, 357-366; c. C. E. Talley, J. B. Jackson, C. Oubre, N. K. Grady, C. W. Hollars, S. M. Lane, T. R. Huser, P. Nordlander and N. J. Halas, *Nano Lett.*, 2005, **5**, 1569-1574.
2. a. J. G. Worden, A. W. Shaffer and Q. Huo, *Chem. Commun.*, 2004, 518-519; b. C.-P. Chak, S. Xuan, P. M. Mendes, J. C. Yu, C. H. K. Cheng and K. C.-F. Leung, *ACS Nano*, 2009, **3**, 2129-2138; c. C. Wang, H. Yin, S. Dai and S. Sun, *Chem Mater*, 2010, **22**, 3277-3282; d. Y. Hu and Y. Sun, *J Am Chem Soc*, 2013, **135**, 2213-2221.
3. a. D.-K. Lim, K.-S. Jeon, H. M. Kim, J.-M. Nam and Y. D. Suh, *Nat Mater*, 2010, **9**, 60-67; b. M. P. Busson, B. Rolly, B. Stout, N. Bonod, E. Larquet, A. Polman and S. Bidault, *Nano Lett.*, 2011, **11**, 5060-5065; c. P. F. Xu, A. M. Hung, H. Noh and J. N. Cha, *Small*, 2013, **9**, 228-232.
4. a. B. Li and C. Y. Li, *J. Am. Chem. Soc.*, 2007, **129**, 12-13; b. B. B. Wang, B. Li, B. Zhao and C. Y. Li, *J Am Chem Soc*, 2008, **130**, 11594-11595; c. B. Li, B. Wang, R. C. M. Ferrier, Jr. and C. Y. Li, *Macromolecules*, 2009, **42**, 9394-9399; d. C. Y. Li, *J. Polym. Sci., Part B: Polym. Phys.*, 2009, **47**, 2436-2440.
5. a. M. Chanana, S. Jahn, R. Georgieva, J.-F. Lutz, H. Baeumler and D. Wang, *Chem Mater*, 2009, **21**, 1906-1914; b. B. Dong, W. Wang, D. L. Miller and C. Y. Li, *J Mater Chem*, 2012, **22**, 15526-15529; c. H. Zhang, B. Dong, T. Zhou and C. Y. Li, *Nanoscale*, 2012, **4**, 7641-7645; d. T. Zhou, B. Wang, B. Dong and C. Y. Li, *Macromolecules*, 2012, **45**, 8780-8789; e. B. Li, B. B. Wang, R. C. M. Ferrier and C. Y. Li, *Macromolecules*, 2009, **42**, 9394-9399.
6. H. Hu and D. L. Dorset, *Macromolecules*, 1990, **23**, 4604-4607.
7. a. M. P. Busson, B. Rolly, B. Stout, N. Bonod, J. Wenger and S. B. Bidault, *Angew. Chem. Int. Ed.*, 2012, **51**, 11083-11087; b. L. Lermusiaux, A. Sereda, B. Portier, E. Larquet and S. Bidault, *ACS Nano*, 2012, **6**, 10992-10998.
8. a. S. Pal, Z. Deng, H. Wang, S. Zou, Y. Liu and H. Yan, *J. Am. Chem. Soc.*, 2011, **133**, 17606-17609; b. J.-H. Lee, J.-M. Nam, K.-S. Jeon, D.-K. Lim, H. Kim, S. Kwon, H. Lee and Y. D. Suh, *ACS Nano*, 2012, **6**, 9574-9584; c. L. Guo, A. R. Ferhan, H. Chen, C. Li, G. Chen, S. Hong and D.-H. Kim, *Small*, 2013, **9**, 234-240.
9. S. K. Ghosh, S. Nath, S. Kundu, K. Esumi and T. Pal, *J. Phys. Chem. B*, 2004, **108**, 13963-13971.
10. R. Sardar, T. B. Heap and J. S. Shumaker-Parry, *J. Am. Chem. Soc.*, 2007, **129**, 5356-5357.